JOURNAL OF MATERIALS SCIENCE 26 (1991) 756–762

The influence of surface melting by CW–CO_2 laser on the structure, composition and stress of the (100) surface of the Fe–17Cr–13Ni alloy

G. MOULIN
Laboratoire de Métallurgie Structurale, ISMA, UA 1107, Bâtiment 413, Université Paris XI, 91405 Orsay, France

During the laser surface treatment, oxidation can take place even with the protection of helium gas. The CW–CO_2 laser melting of the surface does not induce a large distortion of the crystallographic orientation which remains (1 0 0). A misorientation of 3–4 degrees between the melted zone and the unaffected base alloy was measured by Laue diffraction and ion channelling studies. Surface chemical analysis was carried out by X-ray photoelectron and Auger electron spectroscopies in order to obtain information on surface segregation during either the laser cooling, or after annealing up to 850 °C, in $PO_2 = 5 \times 10^{-9}$ Torr. The latter causes segregation of sulphur and/or nitrogen to the surface. This segregation of sulphur and nitrogen is modified between the untreated zone and the treated surfaces (thermal affected zone and melted zone). For instance, on the contrary of nitrogen, the diffusion of sulphur is increased on the melted surface and the activation energy for this diffusion is very dependent upon the defect nature. A difference of nearly 65–70 kJ mol^{-1} is calculated for the enthalpy for the surface segregation of sulphur ΔH^{seg}, between the treated and untreated surface. This difference is only 37 kJ mol^{-1} for nitrogen. In both cases the absolute ΔH^{seg} values are smaller for the treated zone than for the base alloy. A structural study by low electron diffraction (LEED) which gives information on the structure of the surface when clean and in the presence of sulphur and/or nitrogen, shows also the formation of edges, terraces and steps on the treated surfaces. These results are mainly associated with the difference in the content and nature of the defects between the different zones, as observed by scanning electron microscopy analysis or channelling study. Finally a comparison between the mechanical properties of the different zones is made on account of the observation of a linear change of the microhardness on the thermally affected surface. In the thin outer surface zone which is treated by the laser, the stresses associated with the cooling or the isothermal annealing are calculated using formula which associate the stress and the radius of curvature of the sample (from the misorientation which was analysed by ion channelling between the different surface domains). The influence of such an isothermal stress is believed to increase the percentage of vacancies in the melted zone and therefore to modify the activation energy for the diffusion of a substitutional element, such as sulphur. The influence of the elastic energy which is kept during cooling, for example according to the analysis of Evans and Lobb [12], is also discussed.

1. Introduction

The beneficial effect of the melting of steels on wear resistance is usually associated with the homogenization of the solid solution, the formation of cells of small size, the creation of metastable phases (like martensite, nitride . . .) [1]. Residual stresses of several hundreds MPa are measured during such a surface resolidification after the laser melting treatment for both ferritic [2] and austenitic [3] polycrystalline chromium steels. The residual tensile stresses (measured by using the X-ray diffraction peak-shift technique) were nearly the same both along the longitudinal and transverse directions for these rapidly solidified steel surfaces. The implantation of ions, of inert or chemically reactive gases are improved for the wear resistance. Retained austenite or carbide precipitates are used to reduce the crack growth [4].

Too many parameters are then acting for the wear

Part of this work was done in the Laboratoire de Physicochimie des Surfaces, associe au CNRS, ENSCP, Université P et M Curie, 11 rue P et M Curie, 75005 Paris, France.

0022–2461/91 $03.00 + .12

TABLE I Chemical composition of the single crystal alloy (wt %)

Alloy	Element							
	Fe	Cr	Ni	Mo	S	N	O	C
FeCrNi	70.5	16.9	12.6	–	0.0012	0.007	0.0035	0.0014

resistance or surface hardening processes of such industrial polycrystalline steels. A better knowledge of the mechanism of the laser surface treatment needs experiments on laboratory steels without any phase transformation. Recently work has been done on austenitic single crystals of stainless steel. The studies were more specifically related to the lattice disorder evolution with the nitrogen implantation [5] or to the evolution of the surface composition and reactivity with the CW–CO_2 laser surface treatment [6, 7]. The oxidation and element segregation on the surface is not only modified between the laser treated and untreated surfaces, but also between the areas which are rapidly cooled from the melted state (melted zone) and from the solid state (heat-affected zone) (scheme 1). Precisely many laser melt passes are necessary to treat the whole surface of the steel sheets, according to scheme 2.

This study deals with only one laser treatment pass and associates the chemical, structural and mechanical evolutions of the different surfaces (melted, heat affected and untreated ones) with respect to the CW–CO_2 laser surface treatment of a single crystal of Fe–17Cr–13Ni alloy.

2. Materials, heat treatment and experimental procedure

The chemical composition of the alloy is reported in Table I. The crystal was oriented along the ⟨1 0 0⟩ axis by X-ray diffraction, then machined by spark erosion and mechanically and electrochemically polished in 10% $HClO_4$ + 90% $CH_3(CH_2)_3O(CH_2)_2OH$. A further annealing takes place for 5 h at 1000 °C in purified hydrogen.

The laser treatment was performed at the Compagnie Générale d' Electricite (CGE)* using a CW–CO_2 laser. The laser wavelength is 10.6 μm and the laser treatment parameters are reported in Table II.

The segregation treatment took place in the ultra high vacuum chamber of an Auger spectrometer ($PO_2 = 5 \times 10^{-9}$ Torr). Many techniques were used for microstructural, analytical and mechanical purposes: optical microscopy, scanning electron microscopy with dispersive energy or wavelength analyses, X-ray diffraction (Laue method), low energy electron diffraction (LEED) and Auger electron spectroscopy.

TABLE II Conditions for the laser treatment

Power P(KW)	Speed V(cm min^{-1})	Spot size Φ(mm)	Gas
3.0	70	3	He

For the mechanical study, the microhardness was measured using the Vickers method (load = 100 or 200 g).

3. Microstructural and analytical study

3.1. Microstructural study

The Fe–17Cr–13Ni (1 0 0) single crystal sample after the melting treatment is composed of a melted regular section of the surface (MZ) surrounded by two heat-affected zones (HAZ), then with the untreated base

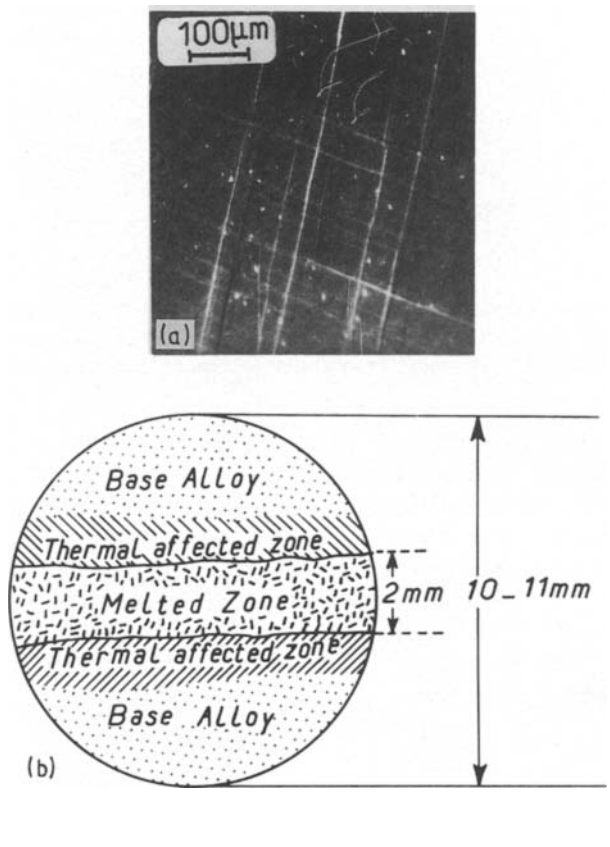

Figure 1 (a) Microstructure observed in the heat-affected zone (b) Scheme 1: Schematic representation of the different surface zones obtained after a CW–CO_2 laser pass. (c) Scheme 2: Different zones after many laser melt passes using a CW–CO_2 laser.

* Laboratoire de Marcoussis de la CGE, CGE, route de Nozay, 91 460 Marcoussis – France.

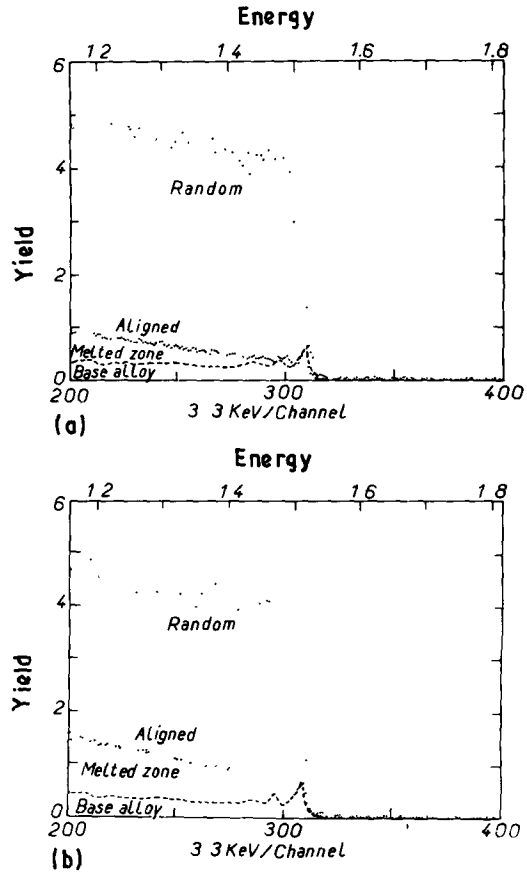

Figure 2 Random and aligned spectra of a 2 MeV He^+ on the (1 0 0) Fe–17Cr–13Ni single crystal for the unaffected alloy (base alloy) and the treated zones (a) melted zone (b) heat-affected zone.

alloy (BA) (scheme 2). There is roughly the same (1 0 0) crystallographic orientation between these three distinct areas and from the two or three first surface layers into the bulk of the alloy. In the heat-affected zone surface slip planes are shown (Fig. 1). Also a small crystallographic misorientation of 4° to 5° is measured between the treated surface and the untreated one, by ion channelling and Laue diffraction. Ion channelling experiments (with ^4He ions at 2 MeV) also provide information on the disorder when compared with the random and aligned spectra (8) (Fig. 2). Then there is an increase in lattice disorder and for disorder viewed along the ⟨1 0 0⟩ direction. This defect increase is higher in the case of the melted surface than in the case of the heat-affected one (within 60%).

3.2. Chemical study

Modifications have recently been shown for the oxidation behaviour of the surfaces during the laser treatment with respect to the surface nature (MZ, HAZ, BA) and to the cooling rate [6]. The oxidized chromium content is higher on the heat-affected zone for the lowest cooling rates.

There is a segregation of sulphur, nitrogen and chromium with a small difference according to the temperature and the nature of the surface. (See for example the case of chromium, sulphur and nitrogen peak heights measured with the Auger spectrometer in Fig. 3a and b.) For instance, the sulphur content is of the order of 0.0020 at% which is higher than the sulphur solubility during the segregation process (for instance 4 p.p.m. at 900 °C [9]). This is the same observation for nitrogen (initial content of 0.0277 at %). The observed saturation of sulphur and chromium, and the high value of $C^{surf}_{S,Cr}$ (0.4 to 0.44 for C^{surf}_{S}; 0.8 to 0.9 for C^{surf}_{Cr} from [7]) with respect to $C^{bulk}_{S\ or\ Cr}$ gives validity to the usual equation for the calculation of the pseudo diffusion parameter D, i.e. $D = \{[C^{surf}_t \times (a/2)]/(2C^{bulk}_{\infty})\}^2 (\pi/t)$ [10, 11] where C^{surf}_t is the surface concentration (atomic fraction) at time t; C^{bulk}

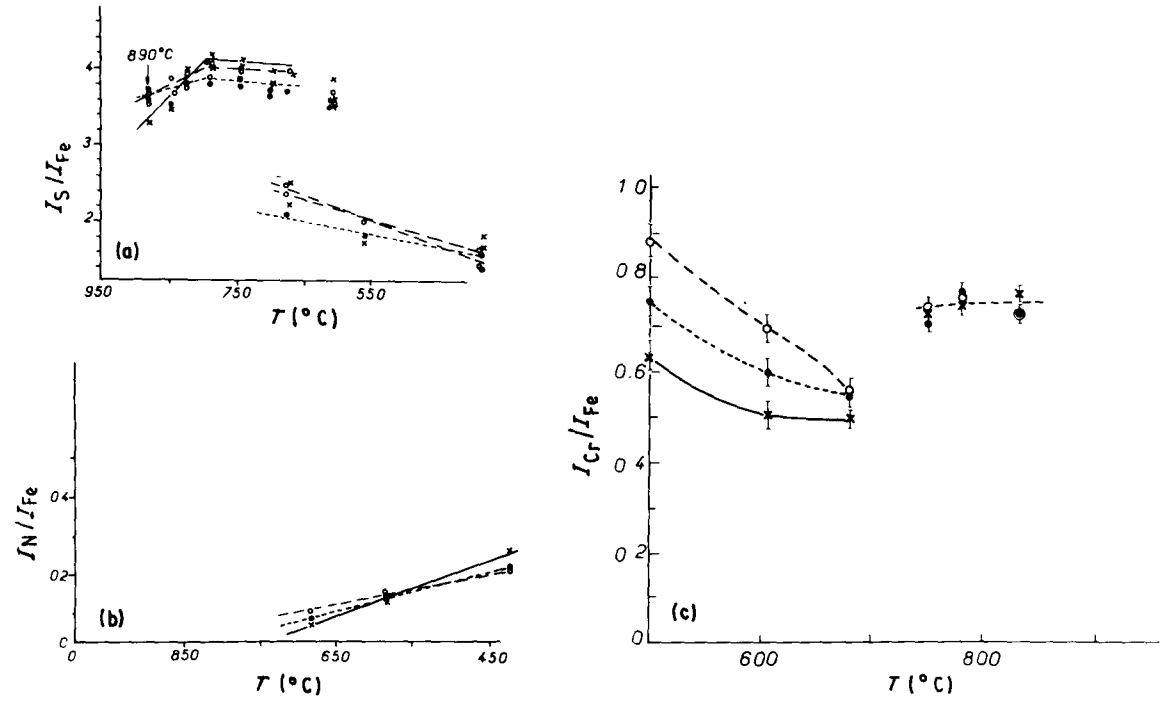

Figure 3 Evolution of the IS/IFe, IN/IFe (a) and ICr/IFe (b) ratios versus the annealing temperature for the different surface zones (× —— × base alloy, ●——● heat-affected zone, ○———○ melted zone), ------ Zemski).

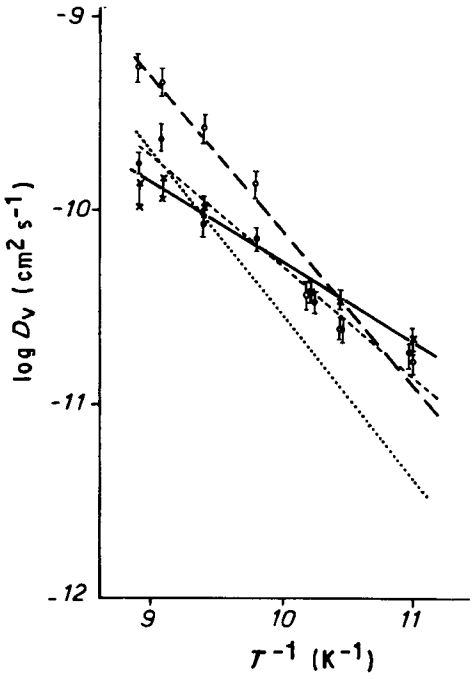

Figure 4 Evolution of the apparent bulk diffusion parameters of sulphur as a function of $1/T$ for the different laser-treated and untreated zones. (×——× base alloy, ●----● thermal affected zone, ○———○ melted zone).

the bulk concentration of the element; $a = 3.578 \times 10^{-8}$ cm the lattice parameter and t = the segregation time.

The different values of D_{Cr} and D_s as a function of the temperature are reported in Figs 4 and 5. The diffusion parameters of sulphur for the base alloy are the same as the literature data [12], but for chromium there is a large increase with respect to the literature

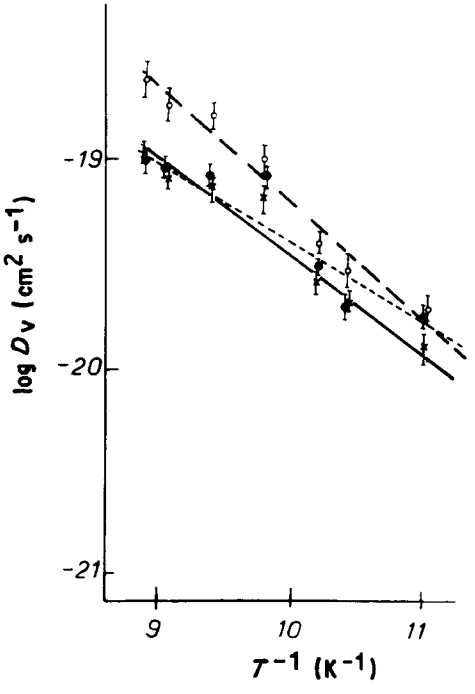

Figure 5 Evolution of the apparent bulk diffusion parameters of chromium as a function of $1/T$ for the different laser-treated and untreated zones. (×——× base metal, ●----● thermal affected zone, ○———○ melted zone).

TABLE III Activation energies (kJ mol^{-1}) for the diffusion of sulphur and chromium on the different surfaces

Surface element	Base alloy	Heat-affected zone	Melted zone
Sulphur	75 ± 4	85 ± 4	146 ± 6
Chromium	100 ± 6	68 ± 4	147 ± 7

data for the bulk diffusion parameters (within a factor 10^2 to 10^3) [13].

The respective activation energy for the diffusion of sulphur and chromium (when sulphur segregates alone on the surface) are reported in Table III.

The activation energies for the diffusion of sulphur and chromium are higher in the melted zone with respect to the two other zones, but the diffusion parameters are enhanced on the melted zone.

Also a modification of the structure of the surface compound is observed by low energy electron diffraction (LEED). First on the surface of the melted and head-affected zones, steps are observed as shown by the elongation of the diffraction spots (Fig. 6) [14]. A nitrogen overlayer structure is also detected on the surface of the base alloy, while this element seems to be randomly distributed on the surface of the treated areas (Fig. 7).

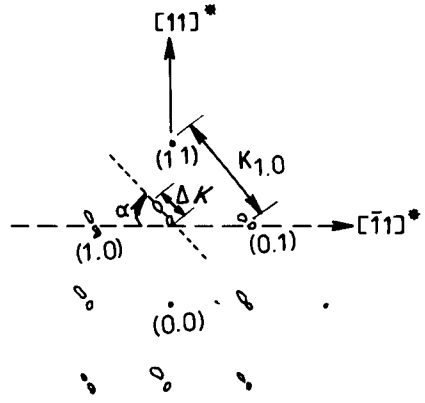

Figure 6 Representation of the LEED pattern of the alloys spots on the laser-treated surface (α is the misorientation angle with respect to the ⟨0 1 0⟩ alloy direction; K the length between the spots and K the length of the double spot associated with the step formation (14).)

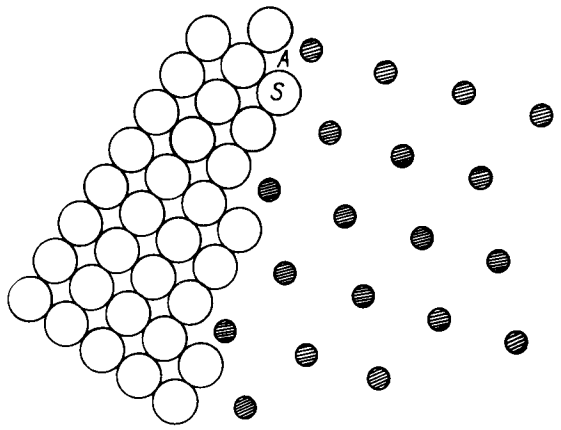

Figure 7 Structure of the two bidimensional adlayers of sulphur and nitrogen on the surface of the untreated alloy ($T < 700$ °C) (A alloy, ○ sulphur, ◎ nitrogen).

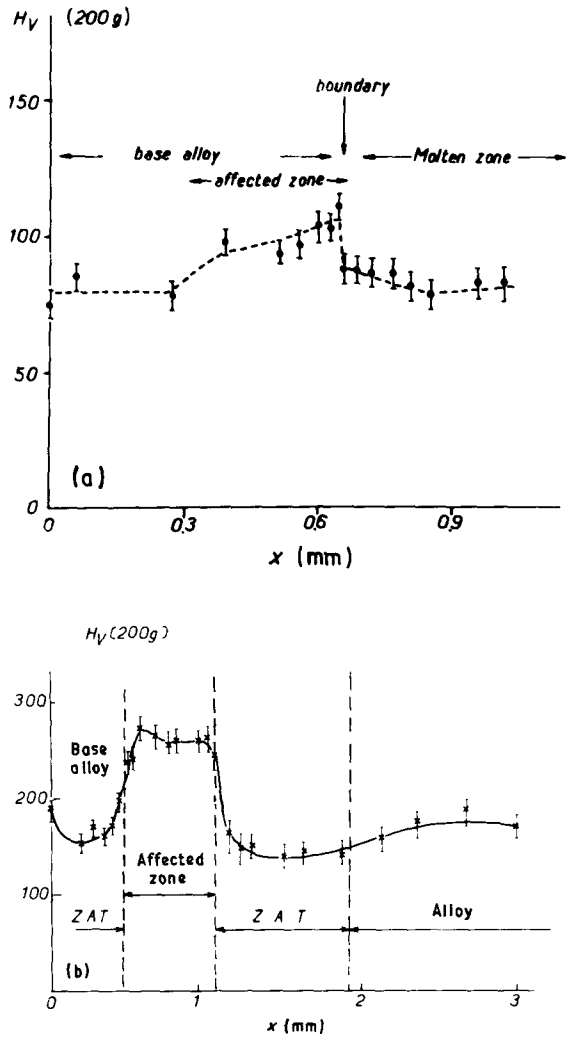

Figure 8 Evolution of the microhardness data from the base alloy to the melted zone in the case of (a) the austenitic Fe–17Cr–13Ni single crystal and (b) the laboratory Fe–17Cr alloy after laser melting treatment.

3.3. Mechanical study

The microhardness data slightly increased (within 20%) in the thermal-affected zone with respect to the melted zone or to the unaffected alloy (Fig. 8a). As a comparison, there is an inverse evolution in the case of a ferritic Fe–17Cr alloy: the microhardness increase takes place straight on the melted surface (Fig. 8b).

4. Discussion

4.1. Determination of the residual stress

As in the case of a deposit on a thin foil [15], the trend of stress with thickness of the laser-treated zone can be studied by observing the direction of bending of such a surface-treated zone. The scheme of Fig. 9 takes into account the different sizes of the treated zones, where d is the thickness of the laser-treated zone; t the thickness of the unaffected alloy, l the length of the sample and r the radius of curvature.

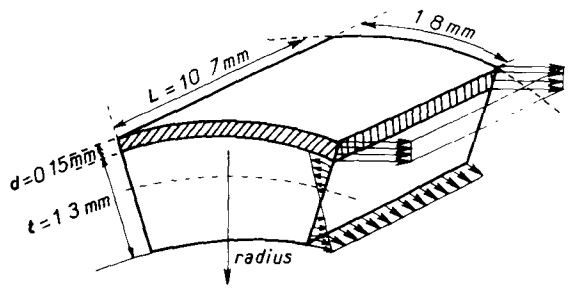

Figure 9 Compressive and tensile stresses (according to the direction of the arrows) in the laser treated alloy allowed to curve after the laser surface melting, then cooling. (d is the thickness of the treated zone; t the thickness of the unaffected alloy; L the length of the sample; r the radius of curvature; and 1.8 mm = width of the treated zones (MZ or HAZ).)

Some formula are obtained from the Brenner and Senderoff analyses [16]. They all assume the following.

(i) The deformation remains an elastic one, because Hooke's law must be used, i.e. $\sigma = E\varepsilon$ (where σ is the stress, ε the deformation and E = Young's modulus).

(ii) There is no stress in the direction perpendicular to the laser-treated surface as mentioned elsewhere [17, 2].

(iii) The stresses are supposed to be nearly isotropic, i.e. quite the same in the longitudinal and transverse directions. Such a result is for instance the case of two ferrous AISI steels as reported in Table IV.

For our experimental conditions, with the same continuous CO_2 laser, isotropic stresses were found for many ferritic and austenitic structures in the case of nickel or cobalt or iron base alloys [18]. For the model of Brenner and Senderoff, two main equations are used.

(i) The first equation states that the sum F of the longitudinal forces within the beam is zero, i.e. that the internal compressive forces are equal to the internal tensile forces: $F = \int \sigma \, dA$ (where σ is the stress from the chosen axis and dA the element of the area of the cross-section).

(ii) The second equation states that the internal bending moment M of the beam is zero about any axis. If the variable y is the distance of the fibres of stress from the chosen axis, $M = \int \sigma y \, dA = 0$. This is the same case as the curvature of a strip that is plated on only one side and is allowed to continuously curve during plating (during the laser surface melting)*. The

TABLE IV Evolution of the residual stress in the longitudinal and transverse directions for the two AISI steels [2]

Sample	Residual stress (MPa)	
	Longitudinal	Transverse
AISI 1018	+ 455 ± 40	+ 395 ± 40
AISI 4140	+ 360 ± 75	+ 145 ± 50

* Indeed a significant error is made for the stress calculation with such a model, because the thickness of the treated zone amounts to more than a few per cent of the thickness of the base alloy. This is required to ensure a complete validity of the model, but here the thickness ratio between the treated surface and the base alloy is ~ 10/100.

formula gives

$$\sigma_1 = [(Et(t + d))/(6d)](1/r)$$

where d is the treated zone thickness; E Young's modulus of the alloy ($= 10.5 \times 10^{10}\,\mathrm{N\,m^{-2}}$); t the base alloy thickness and r the curvature radius. This formula is nearly the same as the relation of Norin [19] in the case of a thin deposit on a thin foil, with $r = l^2/D$ according to the work of Stoney [20] (where l is the thin foil length and D the deflection of the thin foil). The calculated isotropic residual stress is then: $\sigma_1 = 250 \pm 60$ MPa.

4.2. Influence of parameters

4.2.1. Effect of a temperature change

At the melting temperature, when the strip has come to an equilibrium curvature in the treated zone, the effect of the temperature difference ΔT (between the melted zone and the heat-affected one, case 1, or during cooling at room temperature, case 2) would be to alter the curvature. This is also associated with the difference of the expansion coefficients of the alloy (according to the temperature). A modification of the stress, i.e. $\Delta\sigma_T$, is obtained according to

$$\sigma = \{E[t(t + d)]/(6dr)\} - E_c\Delta T(\alpha_b - \alpha_c) \times [t/(t + d)]^2$$

$$\sigma = \sigma_1 - \Delta\sigma_T$$

where t is the thickness of the alloy; d the thickness of the treated zone; E Young's modulus ($10.5 \times 10^{10}\,\mathrm{N\,m^{-2}}$); E_c Young's modulus of the treated zone ($10.5 \times 10^{10}\,\mathrm{N\,m^{-2}}$ at high T, $19.3 \times 10^{10}\,\mathrm{N\,m^{-2}}$ at low T); α_b and α_c are dilatation coefficients according to the temperature ($\Delta\alpha = -0.1 \times 10^{-6}\,^\circ\mathrm{C}^{-1}$).

(i) For case 1, at the melting temperature, $\Delta\sigma_T = 3.6$ MPa.

(ii) For case 2, after cooling from 1200 °C, $\Delta\sigma_T = 21.6$ MPa.

The elastic energy during cooling W^* can also be obtained from a recent formula of Evans and Lobb [21] elaborated in the case of oxide surface layers under equal biaxial stresses

$$W^* = E(1 - \nu)(\Delta T\Delta\alpha)^2$$

where E is Young's modulus; T the temperature difference; $\Delta\alpha$ the difference of the linear expansion coefficients; and ν the Poisson coefficient of the alloy [3]. The elastic energy W^* is found equal to 6.7 kJ mol^{-1}.

All the calculations, then, show a small effect of the temperature change in the residual stress value.

4.2.2. Effect of the physical, structural and chemical parameters

The influence of the elements for the surface strengthening or interstitial solid solution hardening is well known, especially for nitrogen [3]. In the case of these experiments, however, there is no large modification of the surface composition between the different treated and untreated areas. The structure modification for the nitrogen bidimensional compound must be retained between the laser-treated and untreated surfaces. Also the point defect content (vacancies, dislocations) is largely different between the laser-affected and unaffected alloy.

Some physical effects are also discussed in other papers as the chromium oxide volatilization [6] and the mass transport at the surface treated with such a CO_2 laser beam [22]. More particularly the role of the thermocapillarity effect and of the diffusion in liquid state is brought forward.

4.3. Relation between the generated stress and the element diffusion (chromium, sulphur)

Sulphur and chromium are known as located on the substitutional sites of the alloy's net [23]. The enhancement for their diffusion in the treated zone can be associated with the increase of the defect content revealed in the treated zones (especially the melted one) with the channelling experiments (Fig. 2).

For the activation energy of diffusion, the smallest values are obtained in the heat-affected zone (Table III), i.e. in the domain with linear defects (i.e. slip planes). They are effectively known as favourable paths for diffusion [24].

Between the base alloy and the laser-treated alloy there is a nearly constant difference in the activation energies of diffusion of sulphur ($\Delta Q = 70\,\mathrm{kJ\,mol^{-1}}$) (Table III).

The influence of the residual stresses on the diffusion parameters and activation energies for the diffusion could be associated with the evolution of the vacancy nature and content. The relation is for instance shown in the following formula [24]

$$C_1 = C_0\exp[-(E_f + \sigma b^3)/RT]$$

where E_f is the energy for the vacancy formation; σ the residual stress; b the interatomic length and T the temperature.

The additional energetic factor σb^3 for the evolution of the vacancy content is $\simeq 48.5\,\mathrm{kJ\,mol^{-1}}$, i.e. in agreement with the experimental difference for the activation energy between the treated and untreated surfaces. This value is nearly the same as the energy for the formation or migration of vacancies in CFC structures [24].

5. Conclusions

After the melting treatment of a (1 0 0) single crystal of Fe–17Cr–13Ni, the crystallographic orientation remains nearly (1 0 0) within a misorientation of 4° from the laser-treated zone to the unaffected alloy.

Some main results are obtained for the structural and physicochemical behaviour of the laser-treated surfaces. For the segregation process, on all the surfaces there is a competition between the segregation of sulphur and nitrogen below 700 °C. Above this temperature sulphur segregates alone. The chromium content is always higher than in the alloy's bulk. The point defect content is largely increased on the treated surface, especially in the melted area. Also the pseudo diffusion parameters of sulphur and chromium are

enhanced in the melted zone and there is a modification of the structure of the surface layers: steps are observed on the treated surfaces while there is a specific nitrogen bidimensional compound only on the untreated surface.

From the curvature of the surface of the sample after the laser treatment, the residual stress is estimated equal to 250 + 60 kJ mol^{-1} with the formula of Brenner and Senderoff. The effects of the temperature difference between the melted and the heat-affected zones, of the temperature change after cooling do not influence largely the value of the residual stress (3.6 and 21.6 MPa, respectively). The elastic energy during cooling is calculated as 6.7 kJ mol^{-1}.

The other physicochemical parameters are also considered such as

(i) The evolution of the nature and content of the elements on the surface (i.e. as a solid solution or specific compound).

(ii) The mass transport in liquid state at the surface during the laser treatment.

(iii) The evolution of the vacancy nature and content between the treated and untreated surfaces.

Acknowledgements

We would like to thank Dr C. Cohen (Groupe de Physique des Solides, ENS, Paris) for the ion channelling experiments and very fruitful discussions and Dr Com Nougue and Dr Marcus for their help with the laser treatment experiments and discussions.

References

1. K. MONCOFFRE, *Mater. Sci. Eng.* **90** (1987) 99.
2. M R. JAMES, D. S. GNANAMUTHU and R. J. MOORES, *Scr. Metall.* **18** (1984) 357.
3. H. DE BEURS, J A. HOVUIS and J TH M DE HOSSON, *Acta Metall.* **36** (1988) 3123.
4. H. DE BEURS and J TH M DE HOSSON, *Scr. Metall.* **21** (1987) 627.
5. J. L. WHITTON, T LAURSEN, J A NILSON, WING NIP, I. V. MITCHELL, H. H PLATTNER and M L. SWANSON, *Mater. Res. Soc. Symp. Proc.* **41** (1985) 313.
6. G MOULIN, J. M. SIFFRE and P MARCUS, *Mater. Sci. Techn.* **1** (1990) 100.
7. G. MOULIN and P MARCUS, *ibid.* **1** (1990) 107.
8. C. COHEN, *Bull. Soc. Mineral Crystallogr.* **95** (1972) 670
9. N BARBOUTH, M BARBET and J OUDAR, *Mem Et. Sci. Revue de Métallurgie* **4** (1985) 161.
10. D. MACLEAN, "Grain Boundaries in Metals" (Oxford University Press, London, 1957).
11. E. D HONDROS and M P. SEAH, *Met. Trans.* **8A** (1977) 1963.
12. S. V. ZEMSKI, V M. GRUZDENA and L S LVOV, *Izh-Nyssh-Ucheb Zaved, Chern-Met.* **13** (1970) 106.
13. A. F. SMITH, *Met. Sci.* **9** (1975) 375.
14. G MOULIN, V. MAURICE and P. MARCUS *Appl. Surf. Sci.* to be submitted.
15. D. DELAUNAY, A M. HUNTZ and P. LACOMBE, *Corr Sci.* **20** (1980) 1109.
16. A BRENNER and S. SENDEROFF, *J. Res. Nat. Bureau of Standards* **42** (1949) 105
17. V. M MORTON, *Corr. Sci.* **26** (1969) 261.
18. J. HERNANDEZ, E. KERRAND and A. B VANNES, *Mem. et Et. Sci. Rev. Metall.* **10** (1987) 551.
19. A. NORIN, *Oxid. Metal.* **9** (1975) 259.
20. G. C. STONEY, *Proc. R. Soc.* **A82** (1909) 172.
21. H. E. EVANS and R. C LOBB, Proceedings of the 9th International Congress on Metallic Corrosion, Toronto, June 1984 (National Research Council, Canada, 1984) p 46.
22. I B. BOROVSKII, D. D GORODSKII and I M SHARAFEEV, *J. Physique, Colloque C2, Suppl. 2,* **45** (1984) C2–285.
23. N. BARBOUTH and J. OUDAR, *Scr. Metall.* **10** (1976) 415.
24. J PHILIBERT, "Diffusion et Transport de Matière dans les Solides" (Editions de Physique, Paris, 1986) p. 227, 136, 446.

Received 19 October 1989
and accepted 21 December 1989